Supporting Information

Schenk et al. 10.1073/pnas.0908928106

SI Results

Characterization of the HERO Culture System. The HERO culture system allowed hemisphere growth (Fig. S1 *A–C*) and thickening of the cortical wall (Fig. S1 *D–F* and *P*) to proceed in a manner indistiguishable from hemispheres of embryos developed to E15.5 in utero. Accordingly, the increase in (*i*) the proportion of neural progenitors expressing the neurogenic marker *Tis21*-GFP (1, 2) (Fig. S1 *G–I* and *Q*), (*ii*) apical and basal mitoses (identified by phosphohistone 3 immunofluorescence, Fig. S1 *J–L* and *R*), and (*iii*) neurons (identified by β-III-tubulin immunofluorescence, Fig. S1 *M–O*), occurred similarly in 24-h HERO culture as in utero. Thus, with regard to the parameters analyzed, the HERO culture system reproduces cortical neurogenesis and development. Importantly, the direct exposure of neural progenitors to the medium in this system offers 2 decisive advantages with regard to the goal of the present study: first, to explore the possibility of performing pharmacological interference with the actin–myosin system such that INM of APs is inhibited but their progression through the cell cycle, notably cytokinesis, is not; and second, to study INM by BrdU pulse-chase analyses of large populations of APs.

Effects of Various Concentrations of the Nonmuscle Myosin II Inhibitor Blebbistatin on the Cytoarchitecture of the Cortical Wall. We investigated the effects of various concentrations of the nonmuscle myosin II inhibitor Bb (3–6) on the overall morphology and cytoarchitecture of the cortical wall after 24 h of HERO culture. When Bb was applied at 100 μM, 50 μM, or 25 μM of the racemate, the overall morphology and integrity of the cortical wall was grossly perturbed (Fig. S2 *B–D*). Moreover, at these Bb concentrations, cortical cytoarchitecture and neurogenesis were massively impaired, as revealed by immunostaining for the neuronal marker β-III-tubulin and analysis of *Tis21*-GFP expression (Fig. S2 *G–I*). These defects were not observed when the Bb concentration was lowered to 12.5 μM of the racemate (low-Bb treatment), with the overall morphology (Fig. S2 *A* and *E*), cortical cytoarchitecture and neurogenesis (Fig. S2 *F* and *J*; Fig. S3 *M* and *N*) being essentially similar to control.

Effects of Low-Blebbistatin Treatment on Apical Progenitors. Low-Bb treatment for 24 h did not impair the radial morphology of APs as revealed by nestin immunofluorescence (Fig. S4) and the architecture of the VZ as revealed by cadherin immunostaining (Fig. S3 *A* and *B*), nor the apical–basal polarity of APs as indicated by the unaltered appearance of the ZO-1-positive apical junctional complexes (Fig. S3 *C*, *D*, *G*, and *H*).

Double fluorescence of control hemispheres for F-actin (phalloidin, Fig. S3*I*) and for activated nonmuscle myosin II (phosphorylated myosin light chain 2, Fig. S3 *K* and *O*) revealed their relative enrichment at the apical cell cortex. Low-Bb treatment for 24 h altered the apical actomyosin pattern in particular with regard to F-actin staining (Fig. S3 *J*, *L*, and *P*). A reduction in intensity and alteration in pattern of the apical F-actin staining upon low-Bb treatment was observed already after 1 h of HERO culture (Fig. S5). Low-Bb treatment for 24 h resulted in a larger cadherin hole (7) of APs (Fig. S3 *E* and *F*, arrows) and a change of their cell body from an ellipsoid to a more spherical shape (Fig. S3 *A* and *B*, arrowheads), consistent with a relaxation of the actomyosin cell cortex of VZ progenitors that extended from their apical to their lateral side upon inhibition of nonmuscle myosin II.

S Phase of Neural Progenitors Occurs in a Less Basal Location upon Myosin II Inhibition. We investigated the effect of low-Bb treatment on the location of S phase of neural progenitors. To this end, we subjected neural progenitors in HERO culture to low-Bb treatment for 24 h, and identified the position of their S-phase nuclei by a 15-min BrdU pulse at the end of the culture period (Fig. S6*A*). In control cultures, the distribution of BrdU-labeled nuclei peaked in the basal half of the VZ (Fig. S6*B*, *Left*). Low-Bb treatment for 24 h resulted in a shift in the distribution of BrdU-labeled nuclei along the apical–basal axis of the VZ to a less basal localization (Fig. S6*B*, *Right*, and *C*), with the proportion of total BrdU-labeled cells being unchanged by the Bb treatment (Fig. S6*D*).

SI Materials and Methods

HERO Culture and Blebbistatin Treatment. Unless indicated otherwise, C57BL/6 mouse embryos were used. The *Tis21*-GFP knock-in mouse line (2) was maintained as homozygotes in the C57BL/6 background and mated with wild-type C57BL/6 females to obtain heterozygous embryos for the experiments. All experiments were performed in accordance with German and European Union animal welfare legislation.

The HERO culture system established in the present study differs significantly from the whole brain culture and the telencephalic organ culture described previously (8) with regard to parameters such as removal of meninges, culture medium, and mode of culture of hemispheres. Specifically, dissected brains of E14.5 embryos were placed in Tyrode solution at room temperature and cut at the boundary between diencephalon and midbrain, and the diencephalon was removed from the forebrain to obtain the telencephalic hemispheres. During this preparation, the meninges were removed surgically. Hemispheres were transferred to 20-mL glass flasks (1–2 hemispheres per flask) containing 1.5 mL per flask of DMEM/F12 medium supplemented with 1× N2 (Invitrogen), 1× B27 (Invitrogen), and 100 units/mL penicillin/streptomycin (Gibco BRL), and cultured for up to 24 h in a whole-embryo culture incubator (RKI Ikemoto) at 37 °C in an atmosphere of 60% O_2, 5% CO_2, 35% N_2, with continuous rotation at 26 rpm, which ensured flotation of hemispheres.

In Bb experiments, hemispheres were allowed to equilibrate for 30 min under the above conditions and then transferred to flasks with fresh, prewarmed, and oxygenated medium containing 0.1% DMSO and (+/–)Bb as indicated. Bb (Tocris) was dissolved in DMSO (Sigma) and was added from a 12.5 mM stock to the medium to a final concentration of 12.5 μM (0.1% DMSO). Contralateral hemispheres were used as controls.

At the end of HERO culture, hemispheres were fixed for 16 h at 4 °C in 4% paraformaldehyde in 120 mM phosphate buffer pH 7.4. Hemispheres were cryoprotected by incubation for 4 h in 30% sucrose in PBS, embedded in O.C.T. medium (Sakura), and frozen at −20 °C.

BrdU Labeling. For S-phase labeling, 50 μM BrdU (Sigma) was added to the medium during the last 15 min of HERO culture. For cumulative BrdU labeling, 50 μM of BrdU was added to the medium at the beginning of HERO culture, which was then continued for the indicated times up to 22 h. For BrdU pulse-chase labeling, hemispheres preequilibrated in HERO culture were transferred to flasks with medium containing 0.1% DMSO and (+/–)Bb as indicated, and cultured for 15 min. BrdU (50 μM) was added and HERO culture continued for another 15

min, followed by washing of the labeled hemispheres 3 times in Tyrode solution at 37 °C. BrdU-labeled hemispheres were then transferred to fresh, BrdU-free HERO culture medium containing 0.1% DMSO and (+/–)Bb as indicated and chased in HERO culture for up to 14 h.

Immunofluorescence. Immunofluorescence was performed on 10-μm coronal cryosections according to previously described procedures (7), using 0.3% Triton X-100 for permeabilization and incorporating the antigen retrieval steps required for BrdU staining (9) and nuclear transcription factor staining (10), respectively. Primary antibodies used were: goat anti-GFP (MPI-CBG antibody facility, 1:1,000), rabbit anti-phosphohistone 3 (PH3, Upstate, 1:200), mouse anti-β-III-tubulin (Sigma, 1:500), rabbit anti-Tbr1 (Chemicon, 1:500), mouse anti-pan-cadherin (Sigma, 1:200), rabbit anti-ZO-1 (Invitrogen, 1:200), rabbit anti-phospho-MLC2(Ser-19) (Cell Signaling, 1:100), mouse anti-BrdU coupled to rhodamine (MPI-CBG antibody facility, 1:200), rabbit anti-Tbr2 (Chemicon, 1:200), rabbit anti-nestin (Abcam, 1:200) and rabbit anti-Pax6 (Covance, 1:200). Phalloidin coupled to FITC was used to reveal F-actin (Invitrogen, 1:500). Primary antibodies were followed by Cy2-, Cy3-, and Cy5-labeled secondary goat or donkey antibodies (Dianova, 1:1,000). Cryosections were counterstained using 4′,6-diamidino-2-phenylindole (DAPI, Roche, 1:5,000) and mounted in Moviol 4–88. Images were taken with an Olympus BX61 microscope using IPLAB software or a Zeiss LSM confocal microscope, as indicated in the figure legends.

The basal region of the VZ was distinguished from the adjacent SVZ and neuronal layers by (*i*) the shape of nuclei (elongated ellipsoid rather than nearly spherical), (*ii*) the orientation of nuclei (long axis vertical rather than oblique or horizontal), and/or (*iii*) staining of consecutive sections for β-III-tubulin, Tbr1, or Tbr2.

Transmission EM. Hemispheres were fixed for 1–2 h in 4% paraformaldehyde at room temperature and overnight in 2% glutaraldehyde at 4 °C, both in 0.1 M phosphate buffer, pH 7.4. Vibratome sections (200 μm) of the dorsal cortex were cut and processed for EM. The tissue was postfixed with 1% osmium tetroxide and dehydrated through a graded series of ethanol at room temperature (15–30 min for each step) before infiltration with EmBed resin (Science Services) and polymerization at 60 °C for 2 d. Ultrathin sections (70 nm) were cut on a UCT microtome (Leica Microsystems) and viewed in an electron microscope (Morgagni; FEI Company). Micrographs were taken with a charge-coupled device camera (Morada, Olympus) using AnalySis software (Olympus). Interjunctional distance was measured at the apicalmost point of adherens junctions in EM micrographs, using AnalySis software.

1. Iacopetti P, et al. (1999) Expression of the antiproliferative gene TIS21 at the onset of neurogenesis identifies single neuroepithelial cells that switch from proliferative to neuron-generating division. *Proc Natl Acad Sci USA* 96:4639–4644.
2. Haubensak W, Attardo A, Denk W, Huttner WB (2004) Neurons arise in the basal neuroepithelium of the early mammalian telencephalon: A major site of neurogenesis. *Proc Natl Acad Sci USA* 101:3196–3201.
3. Straight AF, et al. (2003) Dissecting temporal and spatial control of cytokinesis with a myosin II Inhibitor. *Science* 299:1743–1747.
4. Kovacs M, Toth J, Hetenyi C, Malnasi-Csizmadia A, Sellers JR (2004) Mechanism of blebbistatin inhibition of myosin II. *J Biol Chem* 279:35557–35563.
5. Limouze J, Straight AF, Mitchison T, Sellers JR (2004) Specificity of blebbistatin, an inhibitor of myosin II. *J Muscle Res Cell Motil* 25:337–341.
6. Ramamurthy B, Yengo CM, Straight AF, Mitchison TJ, Sweeney HL (2004) Kinetic mechanism of blebbistatin inhibition of nonmuscle myosin IIb. *Biochemistry* 43:14832–14839.
7. Kosodo Y, et al. (2004) Asymmetric distribution of the apical plasma membrane during neurogenic divisions of mammalian neuroepithelial cells. *EMBO J* 23:2314–2324.
8. Nomura T, Osumi N (2004) Misrouting of mitral cell progenitors in the Pax6/small eye rat telencephalon. *Development* 131:787–796.
9. Calegari F, Huttner WB (2003) An inhibition of cyclin-dependent kinases that lengthens, but does not arrest, neuroepithelial cell cycle induces premature neurogenesis. *J Cell Sci* 116:4947–4955.
10. Pulvers JN, Huttner WB (2009) Brca1 is required for embryonic development of the mouse cerebral cortex to normal size by preventing apoptosis of early neural progenitors. *Development* 136:1859–1868.

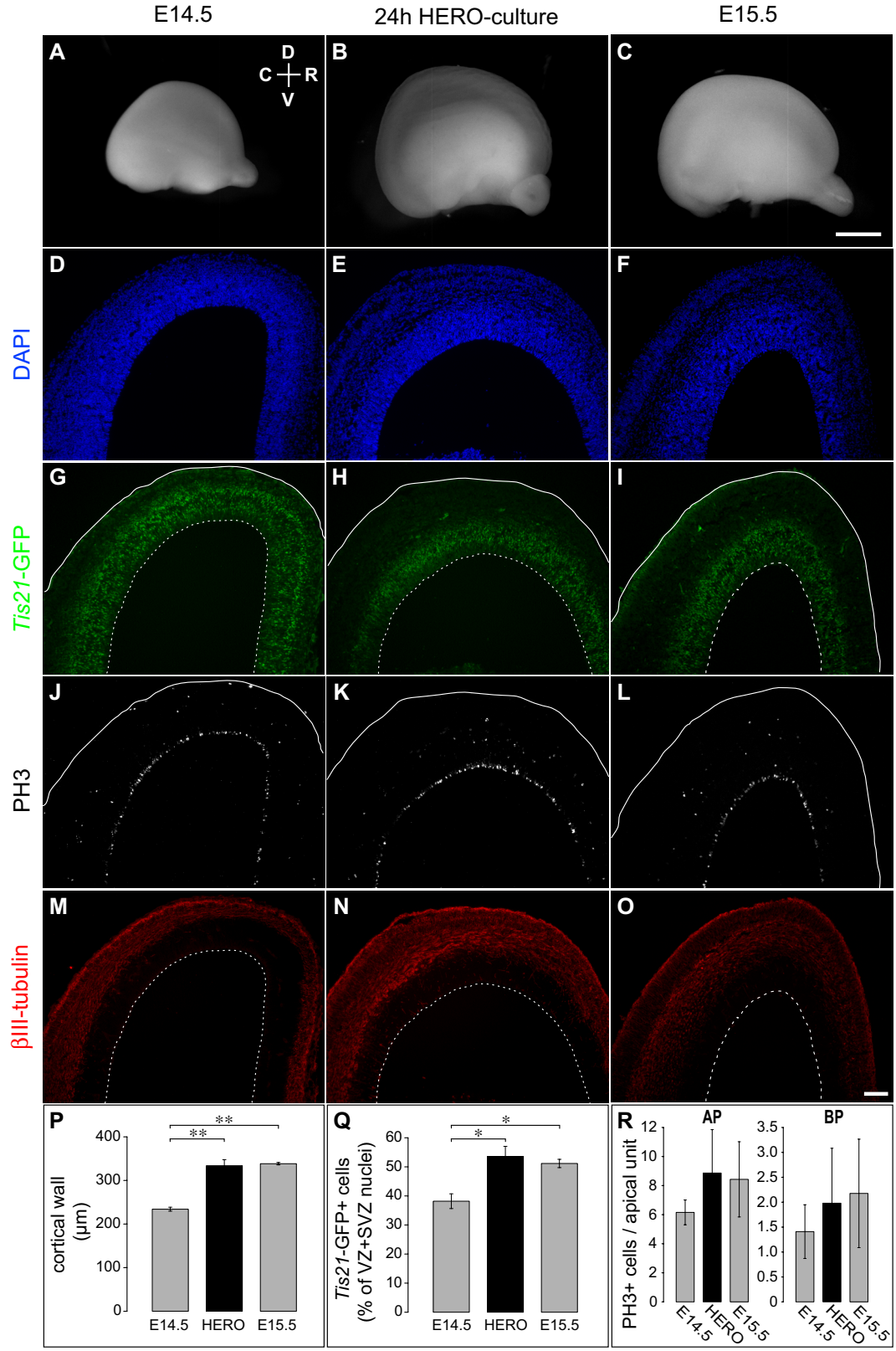

Fig. S1. Characterization of the HERO culture system. (*A–O*) Morphological features of a representative mouse E14.5 hemisphere subjected to HERO culture for 24 h (*B*, *E*, *H*, *K*, and *N*), in comparison to E14.5 (*A*, *D*, *G*, *J*, and *M*) and E15.5 (*C*, *F*, *I*, *L*, and *O*) hemispheres, all from *Tis21*-GFP mice. (*A–C*) Whole-mount view of entire hemisphere after fixation. D, dorsal; V, ventral; R, rostral; C, caudal. (Scale bar, 1 mm.) (*D–O*) Quadruple (immuno)fluorescence for DAPI (*D–E*, blue), intrinsic *Tis21*-GFP (*G–I*, green), phosphohistone 3 (PH3, *J–L*, white), and β-III-tubulin (*M–O*, red). Solid and dashed lines indicate the pial and ventricular surface, respectively. Dorsal is up and lateral is to the left. (Scale bar, 100 μm.) (*P–R*) Hemispheres were treated and analyzed as in *A–O* followed by quantification of cortical wall thickness (*P*); *Tis21*-GFP-positive cells, expressed as percentage of total nuclei in the VZ plus SVZ as revealed by DAPI staining (*Q*); and phosphohistone 3-positive ($PH3^+$) cells, expressed per 100 μm of apical surface. Data are the mean of 3 hemispheres; bars indicate SEM; *, $P < 0.05$; **, $P < 0.01$; number of nuclei and mitoses quantified are given in Table S2.

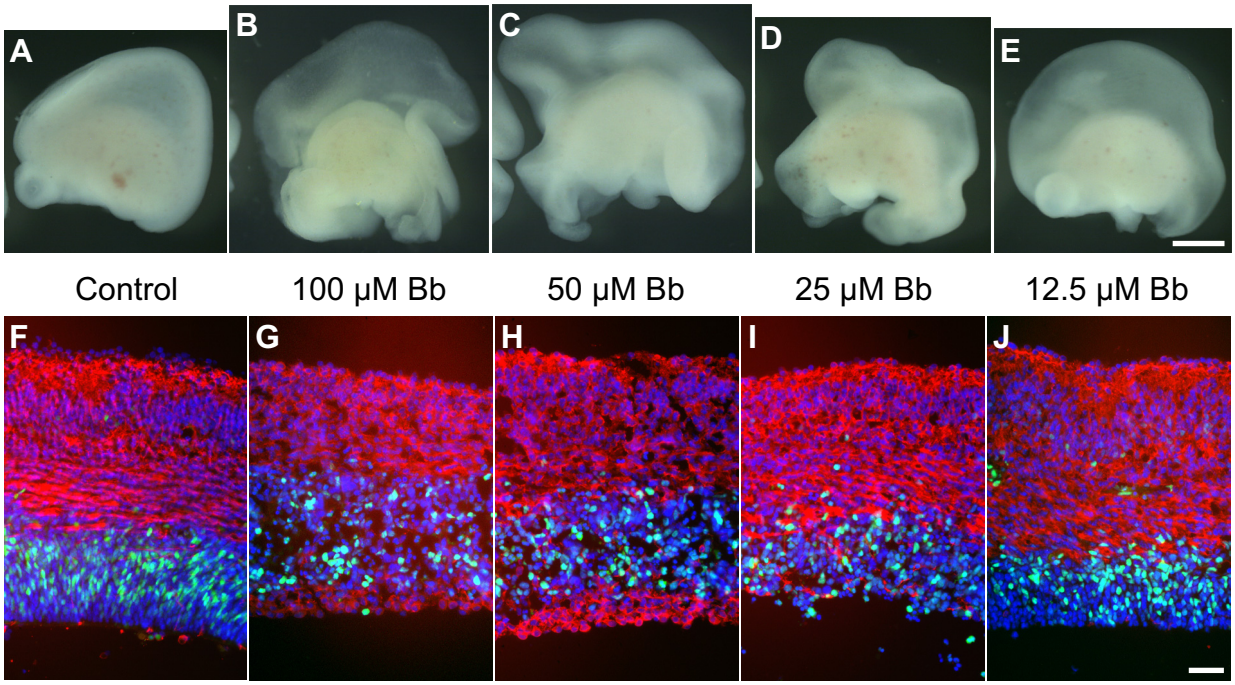

Fig. S2. Effects of various concentrations of blebbistatin on the cytoarchitecture of the cortical wall. Mouse E14.5 hemispheres from *Tis21*-GFP mice subjected to HERO culture for 24 h in the absence (control; *A* and *F*) or presence of 100 μM (*B* and *G*), 50 μM (*C* and *H*), 25 μM (*D* and *I*), and 12.5 μM (*E* and *J*) Bb. (*A–E*) Whole-mount view of entire hemisphere after fixation. Dorsal is up and rostral is to the left. (Scale bar, 1 mm.) (*F–J*) Triple (immuno)fluorescence for DAPI (blue), intrinsic *Tis21*-GFP (green), and β-III-tubulin (red). Ventricular side is down. (Scale bar, 50 μm.)

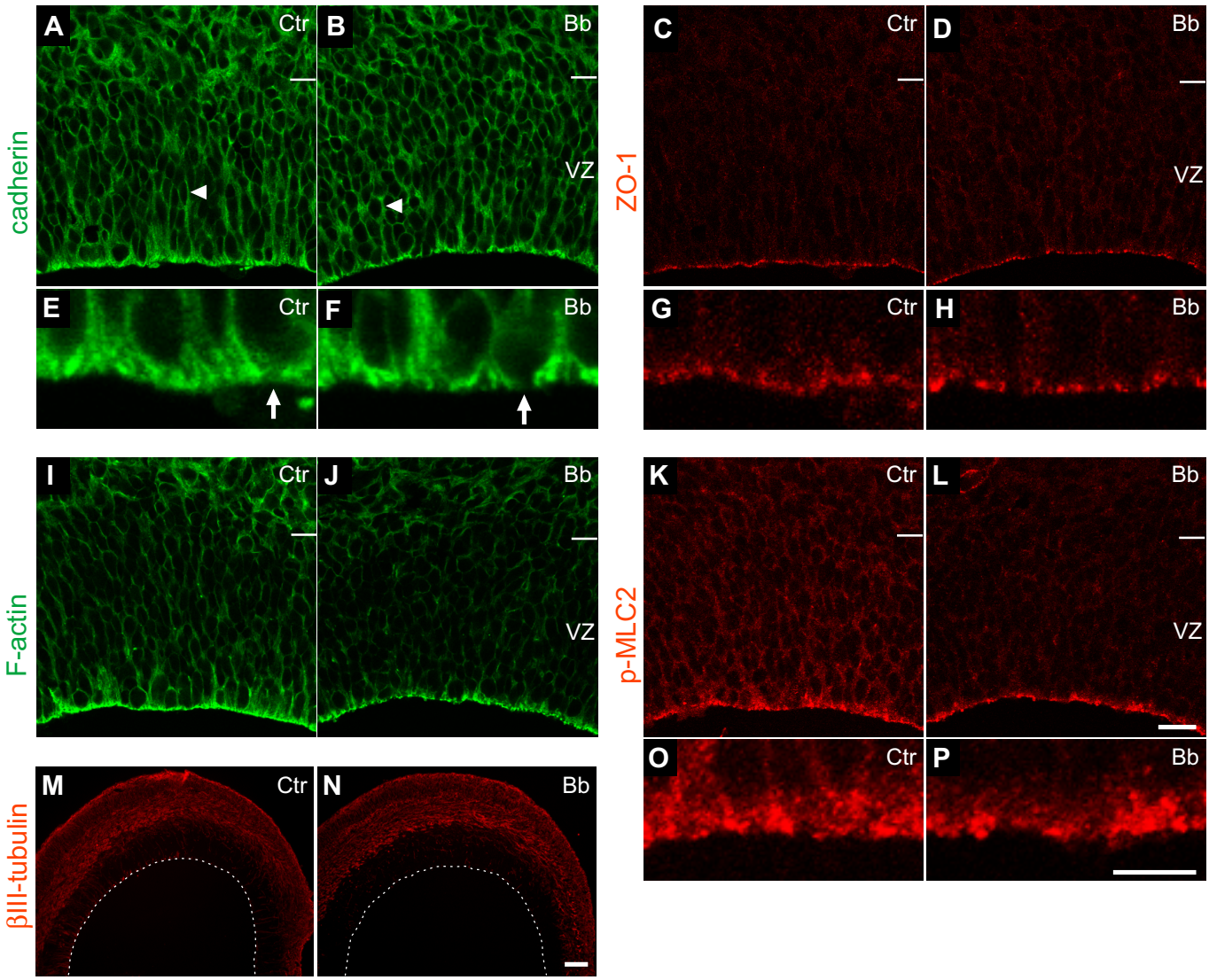

Fig. S3. Effects of low-blebbistatin treatment on apical progenitors. Mouse E14.5 hemispheres subjected to HERO culture for 24 h in the absence (control, Ctr; *A*, *C*, *E*, *G*, *I*, *K*, *M*, and *O*) or presence (Bb; *B*, *D*, *F*, *H*, *J*, *L*, *N*, and *P*) of 12.5 μM Bb. (*A–L*, *O* and *P*) Double (immuno)fluorescence for either cadherin (*A*, *B*, *E*, and *F*, green) and ZO-1 (*C*, *D*, *G*, and *H*, red) or phalloidin (*I* and *J*, green) and phosphomyosin light chain 2 (*p*-MLC2; *K*, *L*, *O*, and *P*, red). All images are 1-μm optical sections. Ventricular surface is down. Arrowheads in *A* and *B* indicate a representative ellipsoid and spherical cell body, respectively. Arrows in *E* and *F* indicate the cadherin hole; note its larger size upon low-Bb treatment. The basal boundary of the VZ is indicated by white lines at the right margins. (Scale bar, 20 μm in *L* and applies also to *A–D* and *I–K*.) (Scale bar, 10 μm in *P* and applies also to *E–H* and *O*.) (*M* and *N*) Immunofluorescence for β-III-tubulin (red). Dashed lines indicate ventricular surface. (Scale bar, 100 μm.)

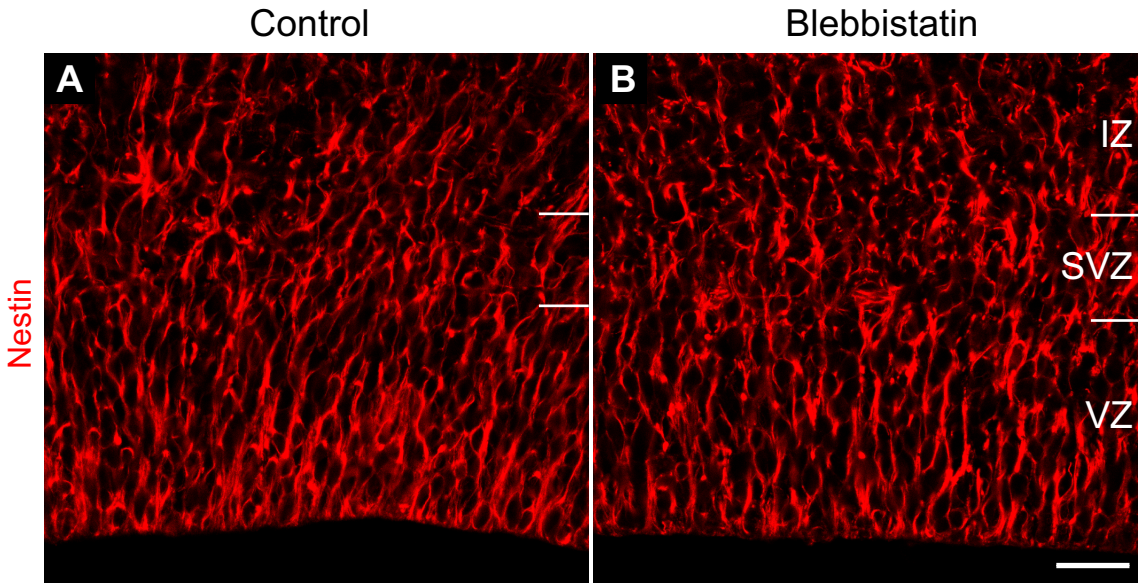

Fig. S4. Low-blebbistatin treatment does not alter the radial morphology of apical progenitors. E14.5 hemispheres were subjected to HERO culture for 24 h in the absence (control) or presence of 12.5 μM Bb, followed by immunofluorescence for nestin (3-μm single optical sections). Ventricular surface is down; boundaries of VZ, SVZ, and intermediate zone (IZ) are indicated at the right margins. (Scale bar, 30 μm.)

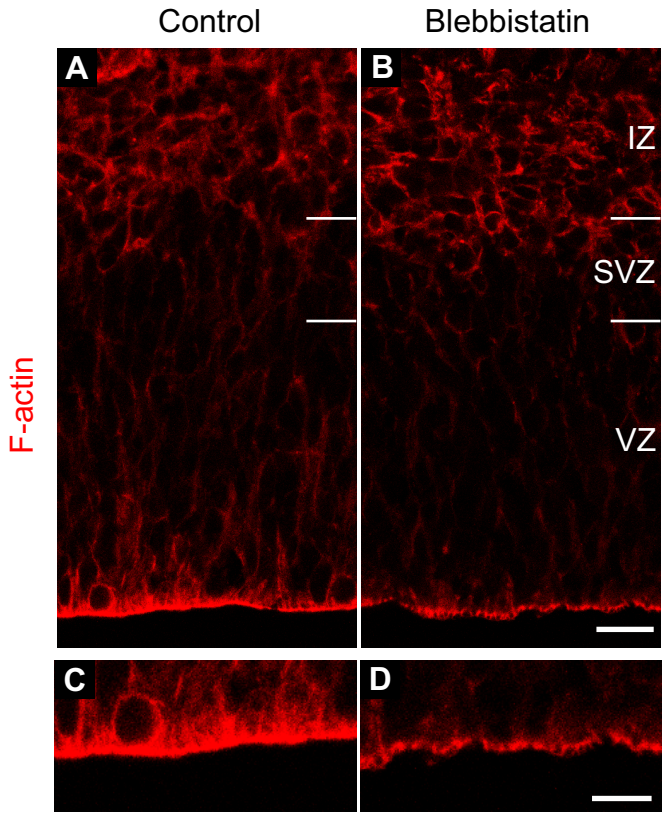

Fig. S5. The alteration in apical F-actin staining is already observed after 1 h of low-blebbistatin treatment. E14.5 hemispheres were subjected to HERO culture for 1 h in the absence (control) or presence of 12.5 μM Bb, followed by phalloidin fluorescence for F-actin (1.5-μm single optical sections). Ventricular surface is down; boundaries of VZ, SVZ, and intermediate zone (IZ) are indicated at the right margins. [Scale bars, 20 μm (*B*) and 10 μm (*D*).]

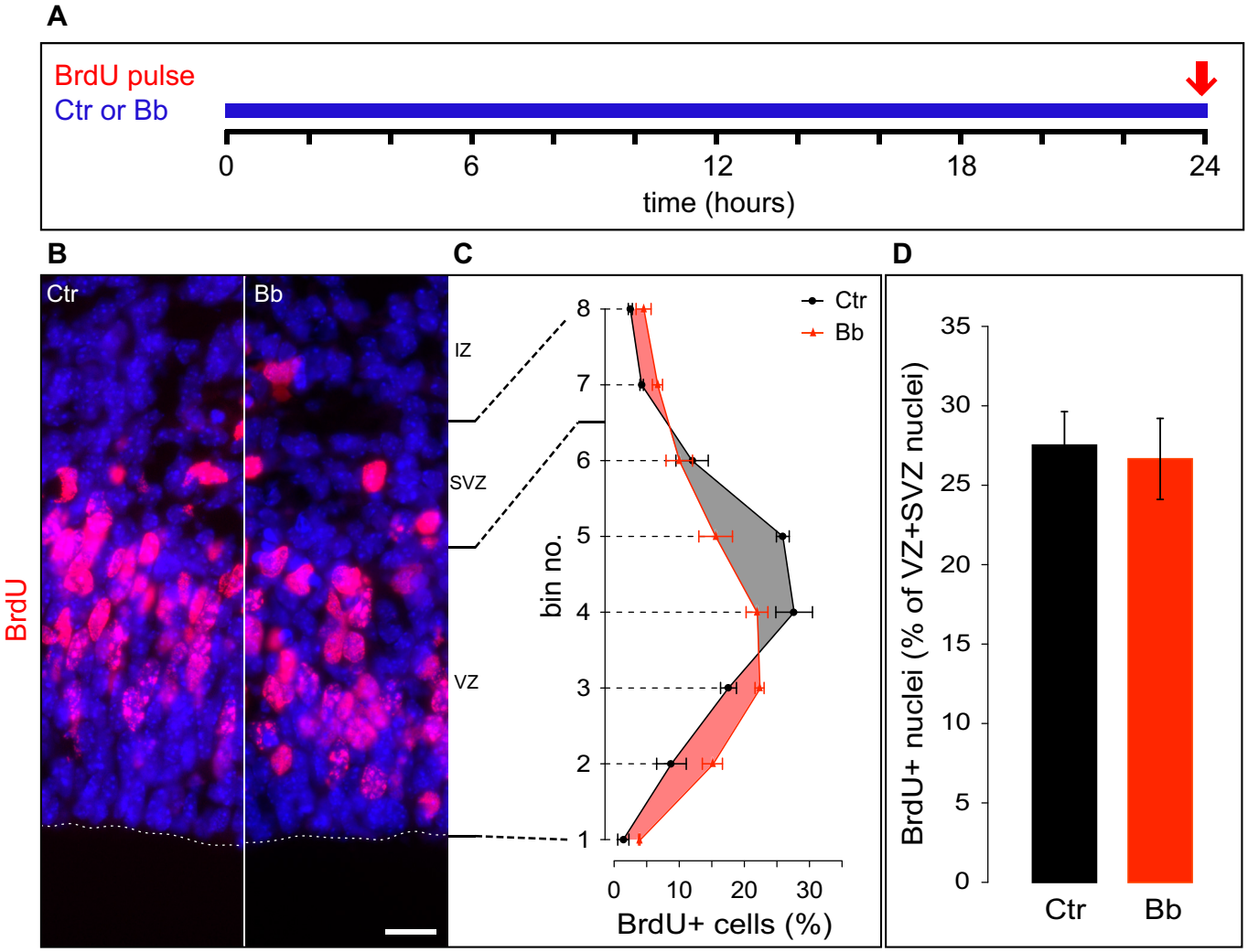

Fig. S6. Low-blebbistatin treatment alters the localization of S-phase nuclei of neural progenitors. E14.5 hemispheres were subjected to HERO culture for 24 h in the absence (control, Ctr) or presence of 12.5 μM Bb (*A*, blue bar), with BrdU being present during the last 15 min (*A*, red arrow), followed by double (immuno)fluorescence for BrdU (red) and DAPI (blue) (*B*). Dashed lines indicate ventricular surface; boundaries of VZ, SVZ, and intermediate zone (IZ) are indicated at the right margin. (Scale bar, 20 μm.) (*C*) Distribution of BrdU-positive nuclei across the VZ plus SVZ, divided into 8 equidistant bins as indicated, with bin no. 1 being at the ventricle and bin no. 8 at the SVZ–IZ boundary. BrdU-positive nuclei in a given bin are expressed as percentage of the total number of labeled nuclei in all 8 bins. Black curve and circles, control (Ctr); red curve and triangles, Bb; differences between control and Bb values are statistically significant (bin no. 5 $P < 0.05$) and are highlighted by black (control > Bb) and red (Bb > control) shading. (*D*) Quantification of BrdU-positive nuclei, expressed as percentage of total nuclei in the VZ plus SVZ as revealed by DAPI staining. (*C* and *D*) Data are the mean of 3 hemispheres; bars indicate SEM. Number of BrdU-labeled (*C*) and DAPI-stained (*D*) nuclei quantified are given in Table S2.

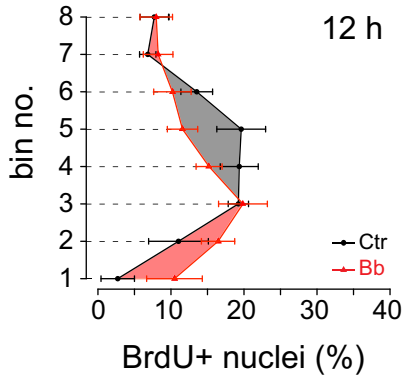

Fig. S7. Low-blebbistatin treatment impairs apical-to-basal nuclear migration/translocation of *Tis21*-GFP-positive progenitors. E14.5 hemispheres from heterozygous *Tis21*-GFP mice in HERO culture were subjected to 15-min BrdU pulse labeling followed by chase for 12 h, in the absence (control, Ctr; black curves) or presence (Bb; red curves) of 12.5 μM Bb. Data show the distribution of BrdU-labeled *Tis21*-GFP-positive nuclei across the VZ plus SVZ (bin analysis and shading as in Fig. S6) and are the mean of 3–4 hemispheres; bars indicate SEM. Ctr and Bb curves are significantly different with a KS *P* value of <0.001. Number of BrdU-labeled *Tis21*-GFP-positive nuclei counted are given in Table S2.

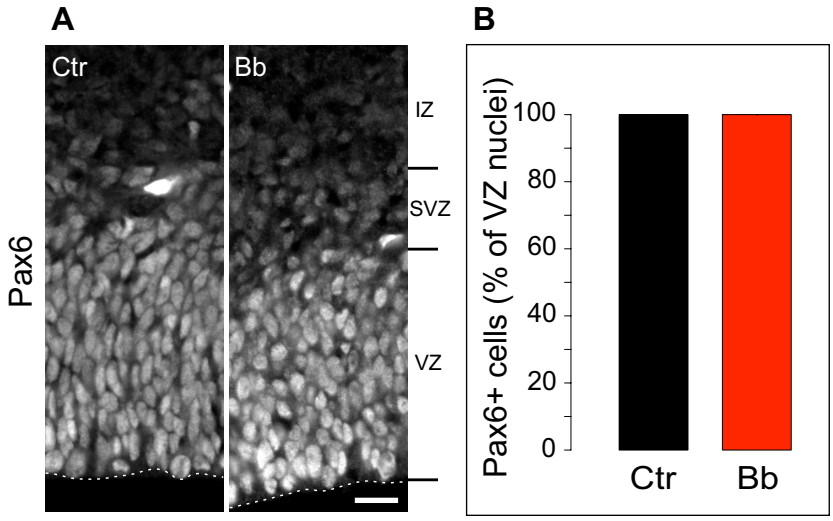

Fig. S8. Low-blebbistatin treatment does not reduce the proportion of Pax6-positive VZ progenitors. E14.5 hemispheres were subjected to HERO culture for 24 h in the absence (control, Ctr) or presence of 12.5 μM Bb, followed by immunofluorescence for Pax6 (*A*). Dashed lines indicate ventricular surface; boundaries of VZ, SVZ, and intermediate zone (IZ) are indicated at the right margin. (Scale bar, 20 μm.) (*B*) Quantification of Pax6-positive nuclei in the VZ, expressed as percentage of total nuclei in the VZ as revealed by DAPI staining. Data are the mean of 3 hemispheres.

Table S1. Cell cycle parameters of control and low-blebbistatin-treated VZ progenitors

Condition	T_C–T_S (h)	T_S (h)	T_C (h)	T_{G2+M} (h)	T_{G1} (h)	GF (% ± SEM)
Control	9.6	4.0	13.6	1.7	7.9	96 ± 1
Blebbistatin	9.3	4.3	13.6	1.7	7.6	96 ± 1

The cumulative BrdU-labeling data shown in Fig. 3*A* were used to calculate the growth fraction (GF) and the length of S phase (T_S) and of the total cell cycle minus S phase ($T_C - T_S$) [Nowakowski RS, Lewin SB, Miller MW (1989) *J Neurocytol* 18:311–318]. The BrdU pulse-chase data of Fig. 3*B* were used to determine the average G2 + M (T_{G2+M}). These data were then used to also calculate the length of the total cell cycle (T_C) and of G1 (T_{G1}).

Table S2. Numbers of cells, nuclei, and mitoses quantified in this study

Figure	Control	Bb	Parameter
1 *E* and *F*	227	202	Interjunctional distance
2*B*	1,261	1,109	BrdU + nuclei
2*D*	1,653	1,502	BrdU + nuclei
2*F*	2,016	1,896	BrdU + nuclei
2*H*	2,502	1,805	BrdU + nuclei
2*J*	2,597	2,051	BrdU + nuclei
2*L*	2,647	2,378	BrdU + nuclei
2*N*	2,468	2,330	BrdU + nuclei
2*P*	2,631	2,065	BrdU + nuclei
3*A*, 1 h	1,064	1,675	DAPI nuclei
3*A*, 5 h	1,683	1,715	DAPI nuclei
3*A*, 9 h	1,986	1,779	DAPI nuclei
3*A*, 14 h	1,902	1,708	DAPI nuclei
3*A*, 22 h	1,336	1,386	DAPI nuclei
3*B*, 1 h	30	40	PH3 + mitoses
3*B*, 2 h	49	60	PH3 + mitoses
3*B*, 3 h	47	43	PH3 + mitoses
3*B*, 4 h	60	51	PH3 + mitoses
3*B*, 6 h	58	35	PH3 + mitoses
4*B*	921	1,360	Tbr2 + nuclei
4*C*	3,463	3,198	DAPI nuclei
4*E*	1,874	1,959	*Tis21*-GFP + nuclei
4*F*	3,945	3,703	DAPI nuclei
4*H*	130	119	PH3 + mitoses
4*I*	2,621	2,677	DAPI nuclei
5*A*	336	356	BrdU + *Tis21*-GFP– nuclei
5*B*	172	438	BrdU + *Tis21*-GFP– nuclei
S1*Q*, E14.5	1,074		DAPI nuclei
S1*Q*, HERO	790		DAPI nuclei
S1*Q*, E15.5	901		DAPI nuclei
S1*R*, E14.5	55		PH3 + mitoses
S1*R*, HERO	88		PH3 + mitoses
S1*R*, E15.5	72		PH3 + mitoses
S6*C*	449	439	BrdU + nuclei
S6*D*	1,633	1,686	DAPI nuclei
S7	666	459	BrdU + *Tis21*-GFP + nuclei